Two- and three-dimensional magnetic order of the rare-earth ions in $R\mathrm{Ba_2Cu_4O_8}$

H. Zhang, J. W. Lynn, W-H. Li, and T. W. Clinton
Center for Superconductivity Research, Department of Physics, University of Maryland, College Park, Maryland 20742 and National Institute of Standards and Technology, Gaithersburg, Maryland 20899

D. E. Morris
Physics Division, Lawrence Berkeley Laboratory, Berkeley, California 94720
(Received 27 December 1989)

Neutron scattering has been used to investigate the magnetic ordering of the rare-earth ions in the $\mathrm{ErBa_2Cu_4O_8}$ and $\mathrm{DyBa_2Cu_4O_8}$ materials. For the Er system a simple three-dimensional (3D) antiferromagnetic structure is observed, in which the magnetic unit cell is twice the chemical unit cell along the a axis, with a Néel temperature $T_N \approx 0.49$ K. In the vicinity of the Néel temperature, however, scattering characteristic of two-dimensional behavior, indicative of the strong anisotropy of the magnetic interactions, is observed. The magnetic anisotropy arises naturally from the crystal structure, as the c-axis spacing of the magnetic ions is ~ 3 times the a-b spacing. 2D behavior is also observed in the Dy material near its Néel temperature of ~ 0.9 K. However, the scattering in the Dy system does not cross over to the expected 3D Bragg peaks at low temperatures, but rather the 2D line shape persists to the lowest temperatures measured. We explain this result as originating from a geometric cancellation of interactions between c-axis layers for the specific Dy a-b spin configuration, which together with the weak intrinsic c-axis interaction renders the *net* interaction along the c axis much smaller than all other known "2D magnets." Hence the 2D and 3D ordering temperatures appear to be quite different for the Dy material. We anticipate that a similar cancellation of interactions is likely to occur in other $R\mathrm{Ba_2Cu_4O_8}$ (R being a rare-earth element) systems.

I. INTRODUCTION

The magnetic properties of the oxide superconductors have been of particular interest for two reasons. One is that the Cu magnetism may be related in a fundamental way to the pairing mechanism in these materials, and the second is that these are ideal systems in which to investigate the behavior of the rare-earth magnetic order parameter and the superconducting order parameter, which should be coupled via the electromagnetic interaction.[1,2] In this latter regard we have been systematically investigating the nature of the rare-earth ordering in the $R\mathrm{Ba_2Cu_3O_{6+x}}$ (R is a rare-earth element) systems, and have found[3,4] that they are prototypical two-dimensional (2D) magnetic systems.[5] We are now extending these measurements to the $R\mathrm{Ba_2Cu_4O_8}$ class of materials, which is similar to the 1:2:3 system except that the (orthorhombic) c axis is approximately twice as long, with two rare-earth ions in the chemical unit cell.[6,7] We find that these 2:4:8 systems also possess highly anisotropic magnetic interactions due to the crystal structure, and consequently they exhibit 2D-like behavior as well. For the Dy material there is an additional cancellation of interactions between c-axis layers, which yields a net interlayer interaction which is exceedingly weak. Hence $\mathrm{DyBa_2Cu_4O_8}$ appears to be the best example of a 2D system found in nature so far.

The magnetic and superconducting properties for both the 1:2:3 and the 2:4:8 materials are quite similar. The rare-earth ions in both systems are electronically isolated from both each other, and from the electrons in the Cu-O layers that superconduct.[7,8] The R-R distance is ~ 3.9 Å in the a and b directions, while the distance along the c axis is ~ 12 Å, and these are basically the nearest-neighbor separations for the rare-earth ions. This crystallographic anisotropy will lead naturally to magnetic interactions which are highly anisotropic. In addition, the low ordering temperatures (~ 1 K) suggest that the exchange interactions are small in the a-b directions and very small in the c direction, leaving the dipole interactions to dominate. In the 1:2:3 materials, considerable evidence has been obtained from specific heat, susceptibility, and directly in neutron scattering experiments, that a 2D description of the magnetism is appropriate, especially in the orthorhombic (and superconducting) systems. In particular, in (superconducting) $\mathrm{ErBa_2Cu_3O_7}$ a rod of scattering characteristic of 2D behavior has been observed,[3] and the order parameter obeys the Onsager[9] solution for the $S=\frac{1}{2}$, 2D Ising model. In this article we report our neutron scattering experiments on the rare-earth ordering in $\mathrm{ErBa_2Cu_4O_8}$ and $\mathrm{DyBa_2Cu_4O_8}$ powders, and we find unambiguous evidence for two-dimensional behavior in both systems. Strikingly, in the case of $\mathrm{DyBa_2Cu_4O_8}$, the sample did not order three-dimensionally even at temperatures far below T_N.

II. THEORETICAL ANALYSIS

A. 3D magnetic diffraction

The magnetic scattering we observe exhibits both 2D and 3D behavior. Since the case of 2D scattering from a

 ©1990 The American Physical Society

powder is somewhat unusual, and because there has been some confusion in the recent literature concerning the relationship between 2D and 3D scattering in these systems, we discuss in some detail here the scattering cross sections expected and the data analysis procedures we have followed.

Consider first the usual situation of 3D magnetic order. Each magnetic ion will magnetically scatter a neutron, and we must coherently add these individual scattered wave amplitudes in order to obtain the total scattering amplitude.[10] The sum usually has the form

$$\sum_{\{R\}} F_M e^{i\mathbf{Q}\cdot\mathbf{R}} , \tag{1}$$

where F_M is the magnetic structure factor for the magnetic unit cell, $\mathbf{Q}$ is the change in the wave vector upon scattering, $\mathbf{R}$ designates the position of each magnetic unit cell, and the sum is over all magnetic cells in the crystal. For all the terms to add coherently, we require that $\mathbf{Q}\cdot\mathbf{R}$ be an integral multiple of 2π for each and every $\mathbf{R}$; this defines the reciprocal lattice vectors τ. The essential point is that since the $\mathbf{R}$ form a 3D lattice, each of the three components of $\mathbf{Q}$ must be restricted to specific values, and this gives rise to the usual Bragg peaks located at the reciprocal lattice vectors τ. Figure 1 shows a representative scattering plane for a system with 3D order. The solid points denote the Bragg points for the case of a single-crystal specimen. To observe a Bragg peak, we must have $\mathbf{Q}=\tau$, that is, the neutron spectrometer must be at the correct scattering angle 2θ [with $|\tau|=4\pi\sin(\theta)/\lambda$], and the sample must be rotated to the proper orientation. A polycrystalline sample, on the other hand, consists of a large number of single crystals, randomly oriented. This has the effect of transforming each Bragg point into a Bragg sphere of radius $|\tau|$, and the projection of these spheres onto the scattering plane yields a series of concentric circles as also shown in Fig. 1. The sample orientation is now irrelevant, and the measured Bragg angle $2\theta_B$ yields $|\tau|$.

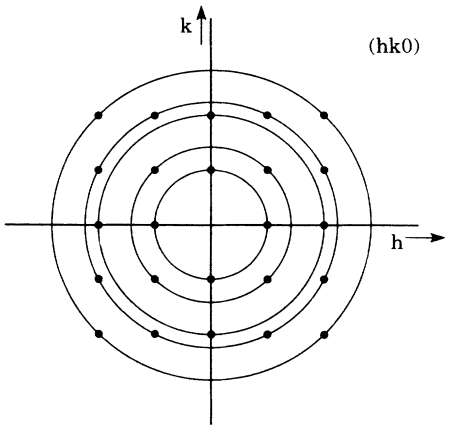

FIG. 1. Schematic representation of the scattering plane, both for a single-crystal sample, and for a powder. The solid points represent 3D Bragg peaks, which is the situation for a single crystal. A powder consists of a collection of single crystals oriented in all possible directions, and the Bragg intensities are distributed on spheres, which appear as circles in this scattering plane.

The integrated intensity for a magnetic Bragg reflection is given by[10]

$$I_M = C\mathcal{M}_\tau A(\theta_B)\left[\frac{\gamma e^2}{2mc^2}\right]^2 \langle 1-(\hat{\tau}\cdot\hat{\mathbf{M}})^2\rangle |F_M|^2 , \tag{2}$$

where the neutron-electron coupling constant in parentheses is -0.27×10^{-12} cm, $\hat{\tau}$ and $\hat{\mathbf{M}}$ are unit vectors in the direction of τ and the spin direction, respectively, and the orientation factor $\langle 1-(\hat{\tau}\cdot\hat{\mathbf{M}})^2\rangle$ must be calculated for all possible domains.[11] C is an instrumental constant which includes the resolution of the measurement. $A(\theta_B)$ is an angular factor which depends on the method of measurement, and $\mathcal{M}_\tau$ is the multiplicity of the reflection. The magnetic structure factor F_M is given by

$$F_M = \sum_{j=1}^{N} \langle \mu_z \rangle_j f_j(\tau) e^{-W_j} e^{i\tau\cdot\mathbf{r}_j} , \tag{3}$$

where $\langle \mu_z \rangle_j$ is the thermal average of the aligned magnetic moment of the magnetic ion at the jth site at position $\mathbf{r}_j$, W_j is the Debye-Waller factor for the jth atom (which is usually neglected at these low temperatures), $f(\tau)$ is the magnetic form factor, and the sum extends over all magnetic atoms in the unit cell. The observed intensity then is directly related to the square of the thermal average of the magnetic moment, $\langle \mu_z \rangle$, which is the order parameter for the phase transition. The preferred magnetic axis ($\hat{\mathbf{M}}$) also can often be determined from the relative intensities. Finally, the scattering can be put on an absolute scale by comparison with the nuclear Bragg intensities,[12] whereby the saturated value of the magnetic moment can be obtained.

The standard technique for identifying the magnetic Bragg scattering is to make one diffraction measurement in the paramagnetic state well above the ordering temperature, and another in the ordered state at the lowest temperature possible, and then subtract the two sets of data.[12] In the paramagnetic state the (free ion) magnetic scattering is given by[10]

$$I_M = \frac{2}{3}\left[\frac{\gamma e^2}{2mc^2}\right]^2 \mu_{\text{eff}}^2 f(Q)^2 , \tag{4}$$

where μ_{eff} is the effective magnetic moment ($=g\sqrt{J(J+1)}$ for a free ion). This is a magnetic incoherent cross section, and the only angular dependence is through the magnetic form factor $f(Q)$. Hence this scattering looks like "background." There is a sum rule on the magnetic scattering in the system, and in the ordered state most of this diffuse scattering shifts into the coherent magnetic Bragg peaks. A subtraction of the high-temperature data [Eq. (4)] from the data obtained at low T [Eq. (2)] will then yield the magnetic Bragg peaks, on top of a deficit (negative) of scattering away from the Bragg peaks. On the other hand, all the nuclear cross sections usually do not change significantly with temperature, and hence drop out of the subtraction. Exceptions to this are if the temperature dependence to the Debye-Waller factor is significant, if there is a structural distortion associated with the magnetic transition such as

through a magnetoelastic interaction, or if the nuclear spins order. In these latter cases polarized beam techniques are needed to unambiguously separate the magnetic and nuclear cross sections.

B. 2D magnetic diffraction

For the case of a 2D lattice the basic sum in Eq. (1) is of course the same, except that the lattice defined by $\{\mathbf{R}\}$ extends in only two directions. In our case this is in the a-b plane, as we assume that the magnetic interactions along the c axis are much weaker than in the planes because of the relative separations of the rare-earth ions. Hence in order to coherently add all the phases we only need to choose the values of Q_x and Q_y appropriately, while the value of Q_z can be anything. This defines a Bragg line or rod, rather than a Bragg point as in 3D. Figure 2 shows a representative reciprocal lattice diagram for this situation. The top portion shows the scattering plane for a single crystal. Note that in order to observe the rod, we can measure at any value of $|\mathbf{Q}|$ we like, as long as we scan through the rod, and as long as $|\mathbf{Q}|$ exceeds the minimum length $|\mathbf{Q}_{\min}|$.

For a powder, we must average the scattering over all possible orientations of reciprocal space. Note that unlike the 3D case, where the Bragg points define discrete spheres, the scattering from the rod is distributed over an infinite range in $|\mathbf{Q}|$; there is a minimum ($|\mathbf{Q}_{\min}|$) below which we will not observe any rod scattering, but there is no maximum. Thus in the powder diffraction case there will be a density of states associated with the rod scattering, as depicted in the bottom portion of Fig. 2. This situation was analyzed by Warren many years ago for the case of x-ray powder patterns of random layered materials.[13] The intensity for the (hk) Bragg reflection is given by[13,14]

$$I_{hk}=C'\left[\frac{L}{\sqrt{\pi}\lambda}\right]^{1/2}\frac{\mathcal{M}_{hk}|F_M|^2F(a)}{(\sin\theta)^{3/2}}\ , \tag{5}$$

where 2θ is the scattering angle, $\mathcal{M}_{hk}$ is the multiplicity of the (hk) reflection, λ is the neutron wavelength, and L is a parameter which represents the size of a domain within the 2D layers. The function $F(a)$ is given by

$$F(a)=\int_0^\infty e^{-(x^2-a)^2}dx\ , \tag{6}$$

where

$$a=(2L\sqrt{\pi}/\lambda)(\sin\theta-\sin\theta_B)$$

and θ_B is the Bragg angle corresponding to $|\mathbf{Q}_{\min}|$. These expressions were convoluted with the instrumental resolution and least-squares fit to obtain the Bragg angle and moment.

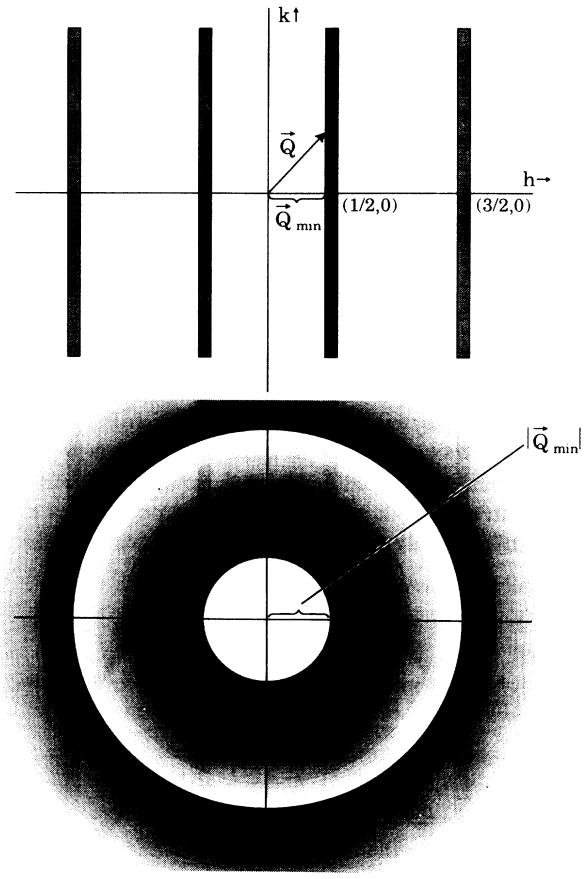

FIG. 2. Schematic representation of the scattering plane for a 2D crystal (top), and a 2D powder (bottom). In the powder the rods are transformed into a density of states for scattering, with the peaks occurring at $|\mathbf{Q}_{\min}|$. In this figure the rods are drawn for the case of $ErBa_2Cu_4O_8$ (or $ErBa_2Cu_3O_7$).

III. EXPERIMENTAL DETAILS

The neutron diffraction experiments were conducted at the research reactor at the National Institute of Standards and Technology. The (unpolarized) neutron diffraction data for both the $ErBa_2Cu_4O_8$ and $DyBa_2Cu_4O_8$ powder samples were taken at the BT-2 triple-axis spectrometer under identical experimental conditions. The incoming neutrons had a wavelength of 2.354 Å defined by a pyrolytic graphite PG(002) monochromator, with a PG filter to suppress higher order wavelength contaminations. Three Söller slit collimators were placed in the beam paths, one before the monochromator, one between the monochromator and the sample, and one after the sample; the collimations were 60′-20′-20′ full width at half maximum (FWHM) acceptance. No analyzer crystal was used. The powder samples were sealed in a flat-plate copper canister of 5 mm thickness with an atmosphere of He exchange gas to promote thermal conduction. A top-loading helium dilution refrigerator was used to cool the samples down to temperatures as low as 50 mK. For each sample, two powder diffraction sets of data were collected over the range of scattering angles from 2° to 62°, one at 50 mK, and another well above the Néel temperature. To isolate the magnetic Bragg peaks from the nuclear Bragg peaks, a subtraction of the high-temperature data from the data at low temperature was taken as explained in the preceding section.

The samples themselves were powders of approximately 10 g each, with (onset) superconducting transition tem-

peratures of ~80 K. The basic 2:4:8 orthorhombic structure (with room-temperature lattice parameters of $a=3.8395$ Å, $b=3.8703$ Å, $c=27.231$ Å (Ref. 7) of the samples was confirmed by our nuclear diffraction data. Details of the sample preparation and phase analysis of these materials are given elsewhere.[7]

IV. RESULTS

A. $ErBa_2Cu_4O_8$ system

The magnetic diffraction pattern for the $ErBa_2Cu_4O_8$ material, obtained by subtracting the scattering observed well above the Néel temperature from the low-temperature data, is shown in Fig. 3. Each data set was counted ~1 min/point, in angular increments of 0.1°. Three strong magnetic peaks are readily identified at scattering angles of 18.36±0.01°, 23.19±0.02°, and 30.76±0.04°, respectively. The error estimates are obtained from fits of Gaussian (resolution) peaks to the data. The three-dimensional spin configuration for the Er moments inferred from these peaks is shown in Fig. 4. In the *a-b* plane, chains of parallel spins occur along the *b* axis, with adjacent chains antiparallel as shown. An identical structure within the *a-b* plane has been observed in the related material $ErBa_2Cu_3O_7$.[3,14,15] The next layer along the *c* axis is obtained by reversing the sense of every moment in the *a-b* plane, and then translating the whole layer by $(b/2)\hat{\mathbf{b}}+(c/2)\hat{\mathbf{c}}$. The three peaks can then be indexed as the $(\frac{1}{2}01)$, $(\frac{1}{2}03)$, and $(\frac{1}{2}05)$ peaks. Six additional (weaker) magnetic peaks could be identified in the data, namely the $(\frac{1}{2}07)$, $(\frac{1}{2}09)$, $(\frac{1}{2}10)$, $(\frac{1}{2}12)$, $(\frac{1}{2}14)$, and $(\frac{1}{2}16)$ peaks. It should be noted that since adjacent layers along the *c* axis are shifted along the *b* axis, but not along the *a* axis, it is a relatively simple matter to distinguish the *a* and *b* axes even though the lattice parameter values are almost the same.

In addition to the basic spin configuration, we also determined the spin direction and the value of the ordered moment of Er. We used the weighted average of the (002) and (100) nuclear peaks to determine the instrumental constant *C*, and least-squares fit Eq. (2) to the seven peaks for which reliable magnetic intensities were

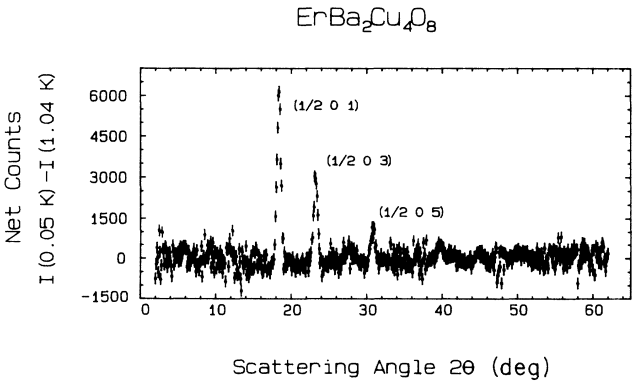

FIG. 3. Magnetic scattering intensity for $ErBa_2Cu_4O_8$ at $T=0.05$ K, which is well below the Néel temperature of 0.49 K.

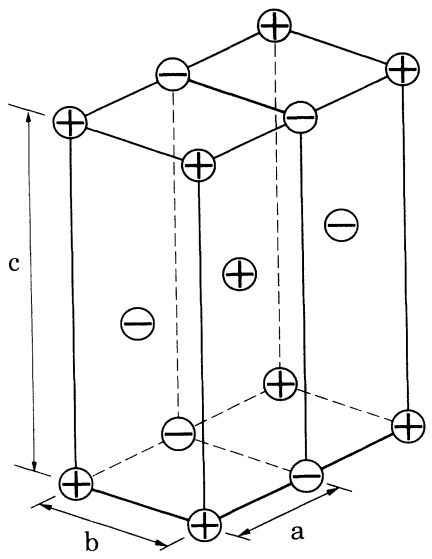

FIG. 4. Ground-state magnetic spin configuration for the Er spins in $ErBa_2Cu_4O_8$. The plus and minus signs represent spins in opposite directions.

obtained, with $\langle\mu_z\rangle$ and the moment direction as variables. A poor fit is obtained if the spin direction is assumed to be along either *a* or *c*, while choosing the *b* axis gives a relatively good fit to the data. A further small improvement of χ^2 was obtained if we chose the spin axis to be ~60° from the *c* axis in *b-c* plane, but we do not consider this to be a significant improvement and take the *b* axis as the likely spin direction. This is the same moment direction as found in the $ErBa_2Cu_3O_7$ system.[3,15] The saturated magnetic moment is then $(3.86\pm0.15)\mu_B$. The experimental intensities and some calculated values are listed in the Table I.

Equations (2) and (3) show that the intensity of the magnetic Bragg peaks is proportional to the square of the ordered moment $\langle\mu_z\rangle$, which is the order parameter (staggered magnetization) for the phase transition. The intensity of the $(\frac{1}{2}01)$ peak as a function of temperature is shown in Fig. 5. The intensity does not change much until the temperature is close to the Néel point, and then it drops quite rapidly. This sharp drop is typical of a 2D-

TABLE I. Observed magnetic intensities for $ErBa_2Cu_4O_8$, compared to the calculated values assuming the spins point along the *b* or *c* axes. The assumption of the *b* axis being the easy direction provides a much better description of the data, and yields a low-temperature moment of $\langle\mu_z\rangle=3.86\mu_B$.

(*hkl*)	I_{obs}	I_{calc} (*b* axis)	I_{calc} (*c* axis)
$(\frac{1}{2}01)$	419±13	381	401
$(\frac{1}{2}03)$	224±13	236	156
$(\frac{1}{2}05)$	93±10	133	51
$(\frac{1}{2}12)$	33±16	36	154
$(\frac{1}{2}14)$	37±14	45	111
$(\frac{1}{2}09)$	27±17	49	7
$(\frac{1}{2}16)$	18±16	47	68

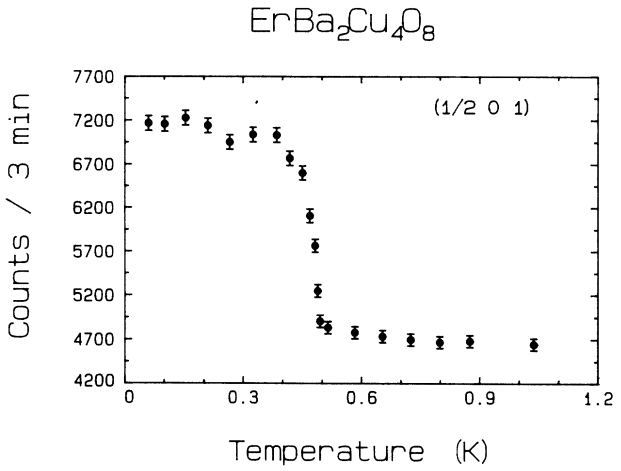

FIG. 5. The magnetic intensity vs temperature for the $(\frac{1}{2}01)$ peak of $ErBa_2Cu_4O_8$. The Bragg intensity is proportional to the square of the sublattice magnetization (order parameter).

like phase transition as recently observed[3] in $ErBa_2Cu_3O_7$. The Néel temperature is determined to be $T=0.49$ K.

At low temperatures most of the magnetic scattering in the system is contained in the Bragg peaks. As we raise the temperature the Bragg intensity will decrease (as illustrated in Fig. 5) at the expense of creating spin-wave excitations. If the magnetic interactions are highly anisotropic as expected, then the lowest energy spin waves will occur in the vicinity of the rods as shown in Fig. 2, and hence we should expect the (energy-integrated) scattering along the rod to strongly increase as the Néel temperature is approached. Figure 6 shows the magnetic scattering observed just at the Néel point, and reveals a skewed line shape characteristic of 2D behavior. The solid curve is a fit to the 2D theory as explained in Sec. II, and the theory provides a good description of the data at this temperature. Hence we conclude that the magnetic interactions along the c axis (J_c) are much weaker than the interactions within the a-b plane (J_{ab}). This will be discussed further in Sec. V.

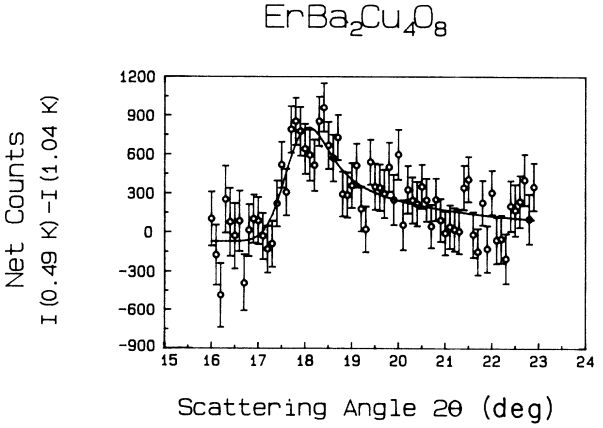

FIG. 6. Magnetic scattering intensity for $ErBa_2Cu_4O_8$ at $T=0.49$ K, just at the ordering temperature. The solid curve is a fit to the 2D theoretical scattering function.

B. $DyBa_2Cu_4O_8$ system

The magnetic diffraction pattern for the $DyBa_2Cu_4O_8$ system was obtained in an identical fashion to the $ErBa_2Cu_4O_8$ sample; data at high temperatures were subtracted from the data obtained at 50 mK. Two portions of the diffraction pattern are shown in Fig. 7. Surprisingly, the scattering at relatively small angles shows a single 2D-like peak, even though we are well below the Néel temperature of ~ 0.9 K (see below). A second 2D magnetic Bragg peak at higher scattering angles is shown in the bottom portion of the figure. The solid curves are again a (single) fit to the 2D theory, assuming long-range order within the a-b plane, and no correlations along the c axis direction. These two peaks correspond to the $(\frac{1}{2}\frac{1}{2})$ and the $(\frac{1}{2}\frac{3}{2})$ rods of a 2D antiferromagnetic spin configuration, shown in Fig. 8. Note that in this 2D structure nearest-neighbor spins are aligned antiparallel, rather than having chains of spins as was the case for the $ErBa_2Cu_4O_8$ (and $ErBa_2Cu_3O_7$) system (Fig. 4). The low-temperature ordered moment was obtained by integrating the magnetic scattering over the angular range corre-

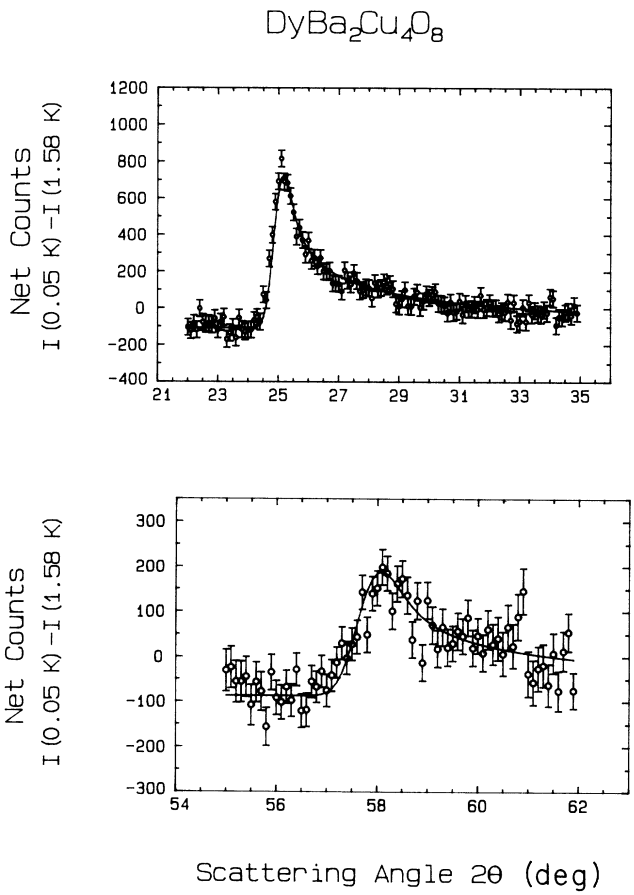

FIG. 7. Magnetic scattering intensity for $DyBa_2Cu_4O_8$ at $T=0.05$ K. The solid curves are the result of a fit to the theoretical scattering expected for a purely two-dimensional magnetic system; top—the scattering profile for the $(\frac{1}{2}\frac{1}{2})$ peak; bottom—the scattering profile for the $(\frac{1}{2}\frac{3}{2})$ peak.

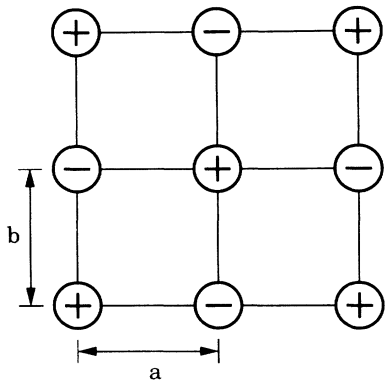

FIG. 8. 2D magnetic spin configuration for the Dy moments within the a-b layers in $DyBa_2Cu_4O_8$. Adjacent layers along the c axis are uncorrelated even well below the 2D ordering temperature.

sponding to one Brillouin zone, and then comparing this intensity to the nuclear Bragg intensities. We obtain a saturated moment of $(5.3\pm0.3)\mu_B$, assuming that the spin direction is perpendicular to the reciprocal lattice vector. The c-axis direction is one obvious choice, which would be consistent with what is known about crystal-field effects in these materials,[16] and with the spin direction observed in the $DyBa_2Cu_3O_7$ system.[17]

Figure 9 shows the intensity at the peak position for the 2D scattering as a function of temperature. The temperature dependence is typical for a magnetic phase transition, except that we are observing a 2D peak rather than a 3D peak as in all the other known examples of 2D magnets. Some rounding is observed in the vicinity of the Néel point, which is typical for the scattering observed in a powder, and we estimate the Néel temperature to be ~ 0.9 K.

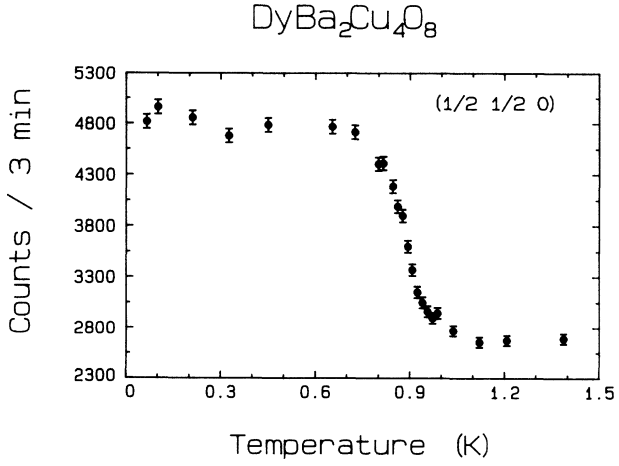

FIG. 9. The intensity of the scattering at the $(\frac{1}{2}\frac{1}{2})$ peak position vs temperature for $DyBa_2Cu_4O_8$.

V. DISCUSSION

The basic rare-earth magnetic orderings which have been observed for the present $RBa_2Cu_4O_8$ materials are quite similar to the $RBa_2Cu_3O_7$ systems, as might be expected since the structures are directly related. In the superconducting phase both are orthorhombic, with the 2:4:8 system having one extra Cu "chain" layer, and with each layer of the rare-earth ions along the c axis being displaced by $b/2$ instead of being directly above as for the 1:2:3 system. The influence of the crystalline electric fields will of course be very important, and we expect the overall splittings in the 2:4:8 systems to be comparable to the 1:2:3 materials (~ 100 meV).[16] For Dy and Er, which have half-integral values of $J=\frac{15}{2}$, each crystal-field level will be (at least) twofold degenerate. Hence the ground state will be magnetic, and likely will be representative of an Ising spin. This is the primary reason why we chose the Er and Dy materials to investigate first.

The results for the $ErBa_2Cu_4O_8$ system are very similar to $ErBa_2Cu_3O_7$. Within the a-b plane the spin structures are identical, and the Néel temperatures are also similar; 0.49 K for $ErBa_2Cu_4O_8$ and 0.618 K for $ErBa_2Cu_3O_7$.[3] The $ErBa_2Cu_3O_7$ has been shown to be a prototypical $S=\frac{1}{2}$, 2D Ising system, and we would expect that the overall behavior of $ErBa_2Cu_4O_8$ would be very similar. Indeed the rapid drop of the order parameter in the vicinity of the Néel temperature is characteristic of a 2D Ising system, and it would be interesting to study this system in more detail if appropriate single crystals become available.

The overall behavior for the $DyBa_2Cu_4O_8$ system is also similar to its sister compound $DyBa_2Cu_3O_7$.[17] The magnetic structure within the a-b planes is again identical for the two systems, and the Néel temperatures are similar; 0.9 K for $DyBa_2Cu_4O_8$ and $\cong 1$ K for $DyBa_2Cu_3O_7$.[17] However, the low-temperature behavior, namely that 2D-like behavior that is observed even at temperatures well below T_N, was somewhat surprising.

To understand why this was unexpected, consider the anisotropy of the magnetic interactions. We designate J_{ab} to be the basic interaction within the a-b plane, which will consist of possible exchange[18] plus dipolar energies, and J_c as the energy (likely dominated by dipolar interactions) of interaction along the c axis. The crystallography for the present 2:4:8 and 1:2:3 systems dictates that $J_{ab} \gg J_c$, and hence the systems should display 2D-like behavior. By this we mean that for $kT \gg J_{ab}$ there will be no significant correlations in the system, and the magnetic (diffuse) scattering will be uniformly spread out over the entire Brillouin zone. As $kT \rightarrow J_{ab}$, strong correlations will develop within the planes, while there will be no significant (dynamic) correlations between layers (see Ref. 3), and this will give rise to a rod of critical scattering. For $J_{ab} > kT > J_c$ we will continue to see a rod of scattering; above the ordering temperature this will be critical scattering, while below the ordering temperature this will consist of very low energy spin waves.

The question is, what determines the ordering temperature, and the crossover from 2D to 3D behavior? For

systems which are strictly two-dimensional, of course, only an Ising model (which we believe to be appropriate for the present materials) will exhibit true long-range order at finite temperature. However, even for the cases of XY or Heisenberg spins, 3D long-range order will be induced even for $J_c \ll J_{ab}$. In the conventional two-dimensional systems such as K_2CoF_4,[19] K_2NiF_4,[20] and more recently $ErBa_2Cu_3O_7$ (Ref. 3) [and of course the Cu spins in La_2CuO_4, Nd_2CuO_4, and $YBa_2Cu_3O_6$ (Ref. 1)], the 2D ordering and the 3D ordering in fact occur at (essentially) the same temperature. The reason for the close proximity of the two transitions is that when the system develops a static moment in the layers, then there is an energy $\pm J_c A^2$ between the layers, where A is the average size of a domain in the layer. The minus sign is for layers that are properly matched (e.g., antiferromagnet configuration if $J_c < 0$) and the plus sign is for layers that are mismatched. Thus even if the interlayer coupling is very weak, there is an energy difference $\sim 2J_c A^2$ between the "correct" and the "wrong" spin configurations, and this energy difference can be quite large, since A is large. Hence as soon as 2D order is established, an ordering should be induced along the c axis, producing 3D Bragg peaks. In the 2D magnets studied to date, in fact, no difference has been discerned between T_N(2D) and T_N(3D).

In the present $DyBa_2Cu_4O_8$ system we have a different situation. Nearest-neighbor spins within the a-b plane form a simple antiferromagnetic arrangement as shown in Fig. 8. In the next layer up along the c axis, all the spins are displaced by $b/2$. For the closest spins between layers, we will have two + spins, and two − spins, and the net interaction is zero by symmetry.[21] Next-neighbor interactions also cancel, and in fact all the (point) interactions sum to zero by symmetry. Hence this is an example of a fully frustrated spin system for the interlayer coupling. Note that in the $ErBa_2Cu_4O_8$ system this cancellation does not occur because of the chainlike ordering in the a-b plane, while in the 1:2:3 systems it does not occur because adjacent layers are not displaced by $b/2$. Finally, we note that if the general similarities between the magnetic structures of the 1:2:3 and 2:4:8 systems hold for the remainder of the $RBa_2Cu_4O_8$ materials, then a similar cancellation of the net interactions along the c axis can be expected since most the $RBa_2Cu_3O_{6+x}$ compounds which have been investigated so far[1] exhibit the same Dy-type spin configuration. A possible exception to this trend may occur for Gd, where the anisotropy is small and an Ising model may not be appropriate. The spin frustration in the 2:4:8 system might then be alleviated by forming a noncollinear structure. Neutron scattering experiments are planned in the near future to investigate this possibility.

In 2D systems like K_2NiF_4 and K_2CoF_4, the nearest-neighbor interactions are comparable in all three directions, but the magnetic structure causes a similar cancellation as for the $DyBa_2Cu_4O_8$ system under consideration here, yielding an effective interaction (via higher order interactions) along the (tetragonal) c axis which is weak and rendering the systems 2D-like. In the $DyBa_2Cu_4O_8$ system the basic (dipolar) interaction along the c axis is itself much weaker than in the a-b plane, and then the cancellation of interactions produces a net c-axis interaction which is extremely weak. Hence in this material the effective coupling between layers relative to the in-plane coupling is much smaller than in any other known system, and it appears that the 2D and 3D ordering temperatures are very different. We remark that with single crystals it is much easier to differentiate between the 2D rodlike scattering and any 3D magnetic Bragg peaks, since they occur at very similar scattering angles but different crystal orientations. It should be particularly interesting to study the critical phenomena of this material in detail when suitable single crystals become available.

ACKNOWLEDGMENTS

The research at Maryland was supported by the National Science Foundation under Grant Nos. DMR 86-20269 and DMR 89-21878.

[1]A review of both theory and experiment that pertains to the oxide superconductors is given in *High Temperature Superconductivity,* edited by J. W. Lynn (Springer-Verlag, New York, 1990).

[2]For a review of magnetic superconductors, see *Topics in Current Physics,* edited by Ø. Fischer and M. B. Maple (Springer-Verlag, New York, 1982), Vols. 32 and 34.

[3]J. W. Lynn, T. W. Clinton, W.-H. Li, R. W. Erwin, J. Z. Liu, K. Vandervoort, and R. N. Shelton, Phys. Rev. Lett. **63**, 2606 (1989).

[4]K. N. Yang, J. M. Ferreira, B. W. Lee, M. B. Maple, W.-H. Li, J. W. Lynn, and R. W. Erwin, Phys. Rev. B **40**, 10 963 (1989).

[5]J. van den Berg, C. J. van der Beek, P. H. Kes, J. A. Mydosh, G. J. Nieuwenhuys, and L. J. de Jongh, Solid State Commun. **64**, 699 (1987); S. Simizu, S. A. Friedberg, E. A. Hayri, and M. Greenblatt, Phys. Rev. B **36**, 7129 (1987); M. W. Dirken and L. J. de Jongh, Solid State Commun. **64**, 1201 (1987).

[6]K. Char, M. Lee, R. W. Barton, A. F. Marshall, I. Bozovic, R. H. Hammond, M. R. Beasley, T. H. Geballe, and A. Kapitulnik, Phys. Rev. B **38**, 834 (1988).

[7]D. E. Morris, J. H. Nickel, J. Y. T. Wei, N. G. Asmar, J. S. Scott, U. M. Scheven, C. T. Hultgren, A. G. Markelz, J. E. Post, P. J. Heaney, D. R. Veblen, and R. M. Hazen, Phys. Rev. B **39**, 7347 (1989).

[8]See, for example, P. H. Hor, R. L. Meng, Y. Q. Wang, L. Gao, Z. J. Huang, J. Bechtold, K. Forster, and C. W. Chu, Phys. Rev. Lett. **58**, 1891 (1987).

[9]L. Onsager, Phys. Rev. **65**, 117 (1944).

[10]See, for example, G. E. Bacon, *Neutron Diffraction* (Oxford, Bristol, 1975).

[11]For simplicity we have assumed that the magnetic structure is collinear, i.e., all the spins point along a common axis.

[12]Additional details can be found in J. W. Lynn, J. A. Gotaas, R. N. Shelton, H. E. Horng, and C. J. Glinka, Phys. Rev. B **31**, 5756 (1985); Q. Li, J. W. Lynn, and J. A. Gotaas, *ibid.* **35**, 5008 (1987).

[13]B. E. Warren, Phys. Rev. **59**, 693 (1941). See also J. K. Kjems, L. Passell, H. Taub, J. G. Dash, and A. D. Novaco, Phys. Rev. B **13**, 1446 (1976), and references therein.

[14]J. W. Lynn, W.-H. Li, Q. Li, H. C. Ku, H. D. Yang, and R. N. Shelton, Phys. Rev. B **36**, 2374 (1987).

[15]T. Chattopadhyay, P. J. Brown, D. Bonnenberg, S. Ewert, and H. Maletta, Europhys. Lett. **6**, 363 (1988); D. McK. Paul, H. A. Mook, L. A. Boatner, B. C. Sales, J. O. Ramey, and L. Cussen, Phys. Rev. B **39**, 4291 (1989); T. Chattopadhyay, P. J. Brown, B. C. Sales, L. Boatner, H. A. Mook, and H. Maletta, *ibid.* **40**, 2624 (1989).

[16]See, for example, U. Walter, S. Fahy, A. Zettl, S. G. Louie, M. L. Cohen, P. Tejedor, and A. M. Stacy, Phys. Rev. B **36**, 8899 (1987); A. Furrer, P. Breusch, and T. Unternahreh, *ibid.* **38**, 4616 (1988); A. I. Goldman, Y. Gao, S. T. Ting, J. E. Crow, W.-H. Li, and J. W. Lynn, J. Magn. Magn. Mater. **76-77**, 607 (1988).

[17]A. I. Goldman, B. X. Yang, J. Tranquada, J. E. Crow, and C.-S. Jee, Phys. Rev. B **36**, 7234 (1987).

[18]The relative contributions of exchange and dipole energies have not been definitively determined in the "magnetic-superconductor" systems. See Ref. 2. L. N. Bulaevskii and A. I. Buzdin, Physica C **153-155** (1988); S. H. Liu, Phys. Rev. B **37**, 7470 (1988).

[19]H. Ikeda and K. Hirakawa, Solid State Commun. **14**, 529 (1974).

[20]R. J. Birgeneau, H. J. Guggenheim, and G. Shirane, Phys. Rev. B **1**, 2211 (1970).

[21]It is easiest to think of a sum of exchange interactions. The dipole-dipole interactions also cancel if the moments point along the *c* axis (which we believe to be appropriate for $DyBa_2Cu_4O_8$), or in fact if they lie anywhere within the *a-c* plane. They also cancel if they point along the *b* axis.